Editorial Manager(tm) for Biomaterials
Manuscript Draft

Manuscript Number: jbmt8709R1

Title: Design of graded biomimetic osteochondral composite scaffolds

Article Type: FLA Original Research

Section/Category: Biomaterials & Tissue Engineering

Keywords: Biomimetic material; Biomineralisation; Chondrocyte; Collagen; Composite; Magnesium

Corresponding Author: Dr. Anna Tampieri, Dr

Corresponding Author's Institution: ISTEC-CNR

First Author: Anna Tampieri, Dr

Order of Authors: Anna Tampieri, Dr; Monica Sandri, Dr; Elena Landi, Dr; Daniele Pressato, Dr; Silvia Francioli, Dr; Rodolfo Quarto, Dr; Ivan Martin, Dr

Manuscript Region of Origin:

Abstract: With the ultimate goal to generate suitable materials for the repair of osteochondral defects, in this work we aimed at developing composite osteochondral scaffolds organized in different integrated layers, with features which are biomimetic for articular cartilage and subchondral bone and can differentially support formation of such tissues.
A biologically inspired mineralization process was first developed to nucleate Mg-doped hydroxyapatite crystals on type I collagen fibers during their self assembling. The resulting mineral phase was non-stoichiometric and amorphous, resembling chemico-physical features of newly deposited, natural bone matrix. A graded material was then generated, consisting of (i) a lower layer of the developed biomineralized collagen, corresponding to the subchondral bone, (ii) an upper layer of hyaluronic acid-charged collagen, mimicking the cartilaginous region, and (iii) an

intermediate layer of the same nature as the biomineralized collagen, but with a lower extent of mineral, resembling the tidemark. The layers were stacked and freeze-dried, to obtain an integrated, monolithic composite. Culture of the material for 2 weeks after loading with articular chondrocytes yielded cartilaginous tissue formation selectively in the upper layer. Conversely, ectopic implantation in nude mice of the material after loading with bone marrow stromal cells resulted in bone formation which remained confined within the lower layer.

In conclusion, we developed a composite material with cues which are biomimetic of an osteochondral tissue and with the capacity to differentially support cartilage and bone tissue generation. The results warrant test of the material as a substitute for the repair of osteochondral lesions in orthotopic animal models.

Ref. Ms. No. jbmt 8709, Design of graded biomimetic osteochondral composite scaffolds

Response to Editor:

1. Please re-format the Abstract as a single paragraph
The change has been introduced

2. In the Materials and Methods, please be consistent with the sub-headings. I assume that all of those you have underlined are of the same level, so in all cases put them on separate lines to the text. As far as possible, try to format each of these sections as single paragraphs
The change has been introduced

3. The same applies to the sub-headings in the Results and Discussion
The change has been introduced**,** as far as possible

4. Re-format the Conclusions as a single paragraph. Do not use capital letters for magnesium and collagen
The change has been introduced

5. Please check the references carefully - you have some major typos (e.g.the journal of ref 1) and some are incomplete (e.g.ref 8). Some do not have paper titles (e.g.29). You are inconsistent with the use of capital letters in titles. Where there are more than six authors, give the names of the first six followed by et al. This section has been compiled very poorly and should be carefully checked.
The references have been carefully checked, completed or modified following the requirements

6. Remove figure 1, and reference to it in the text - it is not necessary
Figures 1 has been removed, and the paper includes now a total of 10 figures.

Response to Reviewer #1:

1) results and discussion should be separated
We would prefer to maintain Results and Discussion combined, in order to avoid possible redundancies and improve readability.

2) figures should be detailed with arrows and information about specific orientations.
Details and arrows have been included in the Figures

3) collagen type 1 was used for the creation of the construct - in every layer? Usually collagen type 1 does not play a role in articular cartilage. This should be addressed in the discussion.
According to the Reviewer's comment, a rationale for the use of type I collagen has been included in the text, as follows: "Type I collagen was selected for the synthesis of the composite layers, including the cartilaginous one, due to (i) its good physico-chemical stability and processability and (ii) high safety and biocompatibility profile, related to the removal of all

telopeptides, which are potentially responsible for immunological reactions." (Section 2.1, Page 2, 1st paragraph). Indeed, type II collagen is normally extracted porcine derivative, and is still not available either in bulk for processing or for clinical use. Nowadays there are only few papers on experimental studies describing the use of type II collagen combined with glycosaminoglycans or different cross-linking agents (Cao H, Xu SY. J Mater Sci Mater Med. 2008 Feb;19(2):567-75). Additionally, using this raw material, the potential risk of immunological reaction still remains unclear.

4) A knitting procedure was applied. could you please give more details. it is not clear how important this technique is for the whole process.
The knitting procedure was introduced to anchor the layers to each other and avoid delamination. The procedure is relatively standard, and a reference has been introduced (Liu C. Xia Z. Pharmaceutical Engineering 85, 1051-64 2007)

5) in figure one all 3 layers are equally thick. if this is true, it does not compare to nature, as you might know. what is your rationale for the three layer structure compared to a 2-layer structure. do you think that gradual biomechanical changes of the implant are important. what happens after cells are grown into the implant. is it still stable compared to the freeze dried status?
In order to address the raised questions, the following phrases have been introduced:

"The thicknesses of the cartilaginous, intermediate and bony layers (respectively about 2.0, 1.5 and 2.5 mm) were selected on the basis of technological limitations (preparations thinner than 1.5 mm are challenging) and of the dimension of native articular cartilage in the sheep joint (selected as in vivo test model)". (Section 2.1, Page 3, 1st paragraph)

"The rationale to fabricate a three-layered scaffold instead of a bi-layered one is based on the consideration that gradual changes in the mechanical features of the external layers, due to different stiffnesses of the differently mineralized fibers, could reduce the mismatch of properties at the interface and increase the composite stability." (Discussion Section 3.3, Page 9, 3rd paragraph)

"The role of 3-layered composites, as compared to 2-layered structures, will also have to be addressed in orthotopic animal models". (Discussion Section 3.3, Page 10, 2nd paragraph)

6) mechanical tests were performed. how many specimen, what kind of test-rationale (numbers/results)?
The flexural strength is measured in 4-pt bending with an upper span of 20 mm, lower span of 40 mm using a crosshead speed of 1 mm/min on specimens with dimensions 7 mm x 4 mm x 60 mm (width x thickness x length). The σ value has been calculated applying the formula $\sigma = 3P_N * a/bd^2$ where P_N is the load in Newton and b and d are respectively the width and the height of the specimen and a is the lower span. (Materials and Methods section 2.2, pag 4)

7) human cells were used for the cartilage layer, bmscs were used fromsheep. why didn't you use either human or sheep? -> discussion

The rationale for the selection of the cell species is now clarified in the Methods section "Cell Isolation and expansion" (Page 4, 3rd paragraph), as follows:

"For the biological validation of the developed composites, we used different cell systems which have been previously shown to efficiently differentiate towards the chondrogenic and osteogenic lineages, i.e. respectively human expanded chondrocytes [17] and sheep bone marrow stromal cells (BMSC) [18]"
The reference n.16, now 18, was substituted with : Mastrogiacomo et al., Biomaterials 2006;27:3230-3237

8) how many specimens were created/implanted in nude mice? numbers are missing. how many animals were used?
The requested details have been included in the Methods section (Page 5, 2nd paragraph), as follows:
"A total of 3 constructs were implanted in 3 different mice."

9) figure 9 should be detailed with arrows etc.
The revised figure (now figure 8) has been modified has recommended

10) In figure 10 there are no chondrocytes as far as I can see. More details on the cell-type should be given. maybe a pathologist or anatomist would help. also the safranin o staining is not clear. could you please add a matrix specific stain like alcian blue.
An inset in the figure has been included to detail the morphological features of chondrocytes and the Safranin O positive matrix (see the revised figure, now Figure 9). The text has also been revised and now reads as follows: "After 2 weeks in chondrogenic medium, cells in the cartilaginous layer displayed a chondrocytic morphology and generated a cartilaginous tissue positively stained for Safranin O (Figure 9c)…." (Page 10, 1st paragraph). Safranin O staining is specific for sulphated glycosaminoglycans present in cartilage, similarly to Alcian blue.

10) -what do you mean by necrotic? do you mean acellular?
The word 'necrotic' has now been revised into 'acellular' (Page 10, 1st paragraph)

11) what is your theory? will the implant be used as a template by the cells and rebuilt? or will the implant survive and be long lasting?
We would predict that the implant will be resorbed and new tissue will form. An ongoing study, referred to in the Conclusions, will address this issue.

*** Mandatory Author Declaration**

AUTHOR DECLARATION

We the undersigned declare that this manuscript is original, has not been published before and is not currently being considered for publication elsewhere.

We wish to confirm that there are no known conflicts of interest associated with this publication and there has been no significant financial support for this work that could have influenced its outcome.

We confirm that the manuscript has been read and approved by all named authors and that there are no other persons who satisfied the criteria for authorship but are not listed. We further confirm that the order of authors listed in the manuscript has been approved by all of us.

We confirm that we have given due consideration to the protection of intellectual property associated with this work and that there are no impediments to publication, including the timing of publication, with respect to intellectual property. In so doing we confirm that we have followed the regulations of our institutions concerning intellectual property.

We further confirm that any aspect of the work covered in this manuscript that has involved either experimental animals or human patients has been conducted with the ethical approval of all relevant bodies and that such approvals are acknowledged within the manuscript.

We understand that the Corresponding Author is the sole contact for the Editorial process (including Editorial Manager and direct communications with the office). She is responsible for communicating with the other authors about progress, submissions of revisions and final approval of proofs. We confirm that we have provided a current, correct e-mail address which is accessible by the Corresponding Author and which has been configured to accept email from biomaterials@online.be.

Tampieri Anna 

Sandri Monica 

Landi Elena 

Pressato Daniele 

Quarto Rodolfo 

Martin Ivan 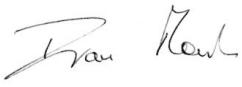

* Title Page

Design of graded biomimetic osteochondral composite scaffolds

Tampieri A., Sandri M., Landi E., Pressato D.[a], Francioli S. [c], Quarto R.[b], Martin I.[c]

Institute of Science and Technology for Ceramic, National Research Council, Via Granarolo 64, Faenza, 48018, Italy

[a] FIN-CERAMICA Biomedical solution SpA, Via Ravegnana, Faenza, 48018, Italy

[b] Advanced Biotechnology Center, Stem Cell Laboratory, University of Genova, Largo R. Benzi 10, Genova, 16132, Italy

[c] Departments of Surgery and of Biomedicine, University Hospital of Basel, Hebelstrasse 20, Basel, 4031, Switzerland

Keywords: Biomimetic material, Biomineralisation, Chondrocyte, Collagen, Composite, Magnesium

Abstract

With the ultimate goal to generate suitable materials for the repair of osteochondral defects, in this work we aimed at developing composite osteochondral scaffolds organized in different integrated layers, with features which are biomimetic for articular cartilage and subchondral bone and can differentially support formation of such tissues. A biologically inspired mineralization process was first developed to nucleate Mg-doped hydroxyapatite crystals on type I collagen fibers during their self assembling. The resulting mineral phase was non-stoichiometric and amorphous, resembling chemico-physical features of newly deposited, natural bone matrix. A graded material was then generated, consisting of (i) a lower layer of the developed biomineralized collagen, corresponding to the subchondral bone, (ii) an upper layer of hyaluronic acid-charged collagen, mimicking the cartilaginous region, and (iii) an intermediate layer of the same nature as the biomineralized collagen, but with a lower extent of mineral, resembling the tidemark. The layers were stacked and freeze-dried, to obtain an integrated, monolithic composite. Culture of the material for 2 weeks after loading with articular chondrocytes yielded cartilaginous tissue formation selectively in the upper layer. Conversely, ectopic implantation in nude mice of the material after loading with bone marrow stromal cells resulted in bone formation which remained confined within the lower layer. In conclusion, we developed a composite material with cues which are biomimetic of an osteochondral tissue and with the capacity to differentially support cartilage and bone tissue generation. The results warrant test of the material as a substitute for the repair of osteochondral lesions in orthotopic animal models.

1. Introduction

Trauma and disease of joints frequently involve structural damage to the articular cartilage surface and the underlying subchondral bone. These pathologies result in severe pain and disability for millions of people world wide and represent a major challenge for the orthopaedic community [1-4]. Even if a series of therapeutic approaches has been developed to treat osteochondral defects, none of them has proved yet to ensure long-lasting regeneration. Considering the intrinsically different biological, biochemical and biomechanical properties of the articular cartilage / subchondral bone system, several groups have directed their efforts into the generation of osteochondral composite materials and/or engineered tissues, using a rather large variety of approaches [5-10]. One of the most promising strategies consists in the generation of heterogenous scaffolds, obtained by the combination of distinct but integrated layers corresponding to the cartilage and bone regions. Such design is based on the recognition of the different requirements to regenerate the cartilage and bone parts of an osteochondral defect, and at the same time prevents the risk of delamination of different components, if these are adjacent but physically separated.

The generation of integrated, bilayered osteochondral scaffolds has been initially proposed using α-hydroxy acids polymers (i.e., poly-lactic acid, poly-lactic-coglycolic acid), combined with a ceramic component (i.e., hydroxyapatite, tricalcium phosphate) in the region corresponding to the subchondral bone [11-12] More recently, biphasic but monolithic materials were formed by joint freeze drying and chemical crosslinking of collagen-based materials (i.e., mineralised or coupled with hyaluronic acid), as well as by ionotropic gelation of alginate-based materials (i.e., containing or not hydroxyapatite ceramic particles), allowing to achieve specific mechanical properties (i.e., elasticity or compression strength) [13].

Along the direction of designing biomimetic osteochondral composite scaffolds resembling the composition of the extracellular matrices of cartilage and bone tissue, in this study we first aimed at further developing a previously reported process of nucleation of hydroxyapatite nanocrystals onto self-assembled collagen fibers [14]. We then generated chemically and morphologically graded hybrid materials, built by stacking a lower mineralised layer produced according to the newly developed technique, an intermediate layer with reduced amount of mineral to mimic the tidemark and an upper layer formed by collagen and hyaluronic acid, reproducing some cartilaginous environmental cues. Finally, we addressed whether the resulting composite materials would differentially support cartilage and bone tissue formation in the different layers, when loaded with articular chondrocytes or bone marrow stromal cells.

2. Materials and Methods

2.1. Material processing and composite development

The organic component, working as matrix mediating the mineralization process, was type I collagen (Coll) extracted from equine tendon, telopeptides free and supplied as acetic gel (an aqueous acetic buffer solution with pH=3.5 containing 1wt% of pure collagen). Type I collagen was selected for the synthesis of the composite layers, including the cartilaginous one, due to (i) its good physico-chemical stability and processability and (ii) high safety and biocompatibility profile, related to the removal of all telopeptides, which are potentially responsible for immunological reactions. The mineral phase, represented by hydroxyapatite (HA) and/or magnesium-hydroxyapatite (MgHA) was directly nucleated onto collagen fibers during their self assembling. Magnesium ions were introduced to increase the physico-chemical, structural and morphological affinity of the composite with newly formed natural bone [15]. In order to generate a scaffold with a morphological and mineralization gradient, three different layers were prepared: a) the upper one, mimicking the cartilagineous layer, and composed of Collagen and Hyaluronic acid; b) the intermediate one, mimicking the tide-mark, and composed of HA/Coll (40/60 wt%) composite; c) the lower one, mimicking the subchondral bone, and composed of HA/Coll (70/30 wt%) composite.

Synthesis of the cartilagineous upper layer: 100 g of 1wt% type I collagen in acid suspension were precipitated by the addition of NaOH (0.1M) solution up to pH 5.5. The precipitate was then washed three times with 300 ml of water. Finally 0.1wt% of hyaluronic acid (HYA: P.M.=1.700.000 uma) was added to the gel just before the crosslinking treatment.

Synthesis of the intermediate bony layer (tidemark): 100 ml of H_3PO_4 (0.040M) solution, mixed with 100 g of 1wt% collagen gel, were dropped in a basic suspension, containing 0.491 g of $Ca(OH)_2$ in 750 ml distilled water to yield a composite HA/Col material in the ratio 40/60wt%.

Synthesis of the lower bony layer: 244 ml of H_3PO_4 (0.040M) solution, added with 70 g of 1wt% collagen gel, was dropped in a basic suspension containing 1.203 g of $Ca(OH)_2$ in 184 ml of distilled water to yield a composite HA/Col material in the ratio 70/30 wt%. The same mineralization process was also performed to nucleate Mg doped HA on collagen fibers. In particular, 244 ml of H_3PO_4 (0.040M) solution, mixed with 70 g of 1wt% collagen gel, were dropped in a basic suspension containing 1.203 g of $Ca(OH)_2$ and $MgCl_2$ in 184 ml of distilled water. The amount of $MgCl_2$ was calculated to obtain a molar ratio X_{Mg} (Mg/Ca) = 5% in the mineral phase. The drop wise addition procedure was performed under stirring and assuring a slow decrease of pH [14] up to neutrality (total dropping time for the considered volumes ~30 min.).

Each synthesized material was treated with the crosslinking agent 1,4-butanediol diglycidyl ether (BDDGE) through immersion for 48 hours in a BDDGE aqueous solution (2.5 mM), setting up a BDDGE/collagen ratio equal to 1wt%. After this cross-linking treatment, each preparation was filtered and layered on Mylar sheet. The thicknesses of the cartilaginous, intermediate and bony layers (respectively about 2.0, 1.5 and 2.5 mm) were selected on the basis of technological limitations (preparations thinner than 1.5 mm are challenging) and of the dimension of native articular cartilage in the sheep joint (selected as in vivo test model). The three layers were piled up, then a knitting procedure [16] was applied at each interface (bone-tidemark interface and tidemark-cartilage interface) to assure good integration by the exchange of anchor fibers between the layers and avoid delamination at the interface. Finally, freeze-drying with a controlled freezing and heating ramp was performed from 25°C to -25°C and from -25°C to 25°C in 50 min., under vacuum conditions (P = 0.20 mbar) .

2.2 Composite characterization

ICP-OES quantitative analysis, using an inductively coupled plasma - atomic emission spectrometry (ICP-AES: Liberty 200, Varian, Clayton South - Australia), was applied to determine the content of Mg^{2+}, Ca^{2+}, PO_4^{3-} ions constituting the mineral phase forming the composites. Samples were previously prepared using an acid attack (nitric acid 65wt%). The obtained values were expressed in term of Ca/P and Mg/Ca molar ratios. The composites were examined by scanning electron microscopy (ESEM) (Quanta 600 FEG, FEI Company, Hillsboro, OR) equipped with EDS (analyzing program: EDAX Genesis, Mahwah, NJ). Infrared spectroscopy (FTIR) was performed by using a Nicolet 4700 Spectroscopy on pellets (13 mm ∅) which were prepared by mixing 2 mg of ground sample with 100 mg of KBr in a mortar and pressing. Collected X-ray diffraction patterns were recorded by a Bruker AXS D8 Advance instrument in reflection mode with Cu-K_a radiation and by a Rigaku Miniflex diffractometer (Cu-K_a radiation). The samples were ground through a cryo-milling apparatus to obtain relatively uniform particle size powder. Observations of composites materials by transmission electron microscopy (TEM) were performed with a JEOL EX4000 instrument with acceleration potential of 400 kV. Samples were dispersed on lacy carbon Cu grids by contact with the grids and subsequent gentle shaking.

Enzymatic tests were performed on mineralized and non-mineralized materials using 200 U/ml of Collagenase solution (in 0,1 M Tris-HCl pH=7.4). The kinetics of enzymatic degradation was followed by an UV-visible spectrophotometer, that allowed to observe the different absorbance in function of time. At $\lambda = 280$ nm the absorption of the aromatic amino-acids tyrosine and tryptophan occurs and it is possible to estimate the increase of concentration of degraded collagen in solution.

Solid state ^{13}C NMR spectra were performed at 50.33 MHz on a Bruker AC-200, equipped with an HP amplifier. Samples were finely powdered and packed into 4 mm zirconia rotors and sealed with Kel-F caps.

Mechanical tests were performed on mineralized specimens (bars 3mm x 7mm x 60mm) obtained through cold uni-axial pressing at different pressures of freeze dried HA/Coll 70/30 composite materials and having different final porosities. Three specimens have been prepared for each pre-selected porosity (in the range 45-65 vol%). Young's Modulus was measured by resonant frequency method using an H&P gain phase analyzer (Yokogama, Hewlett Packard, Tokyo, Japan) and flexural strength σ through the 4-point (lower span = 40mm, upper span = 20 mm) bending method (Instron machine model 1195, High Wycombe, Bucks, UK) using a crosshead speed of 1mm/min. The σ value has been calculated applying the formula $\sigma = 3P_N * a/bd^2$ where P_N is the load in N and b and d are respectively the width and the height of the specimen and a is the outer span.

2.3 Cell isolation and expansion

For the biological validation of the developed composites, we used different cell systems which have been previously shown to efficiently differentiate towards the chondrogenic and osteogenic lineages, i.e. respectively human expanded chondrocytes [17] and sheep bone marrow stromal cells (BMSC) [18].

Full-thickness human articular cartilage biopsies were obtained post mortem (within 24 h after death) from the lateral condyle of knee joints of 2 individuals with no history of joint disease, after informed consent by relatives and in accordance with the local ethics committee of University Hospital Basel, Switzerland. Cartilage tissue was minced, digested with 0.15% type II collagenase (10 mL solution/g tissue, 300 U/mg, Worthington Biochemical Corporation, Lakewood, NJ) for 22 hours and the isolated chondrocytes resuspended in Dulbecco's modified Eagle's medium containing 10% fetal bovine serum, 4.5 mg/mL D-glucose, 0.1 mM nonessential amino acids, 1 mM sodium pyruvate, 100 mM HEPES buffer, 100 U/mL penicillin, 100 µg/mL streptomycin, and 0.29 mg/ml L-glutamine (*complete medium*). Chondrocytes were expanded in *complete medium* with the addition of 1 ng/ml of transforming growth factor-b1, 5 ng/ml of fibroblast growth factor-2 and 10 ng/ml of platelet-derived growth factor-bb in a humidified 37°C/5% CO_2 incubator, as previously described [17]. BMSC were obtained from sheep iliac crest marrow aspirates of 3 year old ewes. All procedures were approved by the Institutional Ethical Committee. BMSC were cultured as described [18]. Mononuclear cells were plated at $5x10^6$ in 100mm dishes in Coons modified Ham's F-12 medium supplemented with 10% FCS and 1ng/ml human recombinant FGF-2 (Austral Biologicals, San Ramon, CA). Medium was changed after 3 days and twice weekly.

2.4 Generation and culture of chondrocyte-scaffold constructs

Expanded human articular chondrocytes were resuspended at a concentration of $2x10^8$ cells/mL and aliquots of 80µl (i.e., $1.6x10^7$ cells) were statically loaded onto the composite scaffolds (8mm diameter, 6 mm height disks), either from the cartilaginous or from the subchondral bone layer. Chondrocyte seeded scaffolds were then transferred to agarose-coated dishes and cultured for two weeks in *complete medium* supplemented with 0.1mM ascorbic acid 2-phosphate, 10µg/mL insulin and 10ng/mL TGFβ3 (*chondrogenic medium*), with medium changes twice a week.

2.5 Generation and implantation of BMSC-scaffold constructs

Expanded sheep BMSC were resuspended at a concentration of $2.0x10^7$ cells/mL and aliquots of 100µl (i.e., $2.0x10^6$ cells) were statically loaded onto the composite scaffolds (8mm diameter, 6 mm height disks), both from the cartilaginous and from the subchondral bone layer. BMSC/scaffold composites, in agreement and with the approval of the competent ethical committee and legal authorities, were subcutaneously implanted in immuno-deficient (ID) (CD-1 nu/nu) mice by using an established model of ectopic bone formation [18]. Recipient ID mice of 1 month of age, purchased from Charles River Italia, were kept in a controlled environment and given free access to food and water. Mice were anesthetized by intramuscular injection of Xilazine (20 µg/ml) and Ketamine (30 µg/ml). Bioceramic/BMSC composites were implanted subcutaneously on the back of the mice. A total of 3 constructs were implanted in 3 different mice. Animals were sacrificed 8 weeks after implantation. Grafts were harvested and processed for histological analysis.

2.6 Histological characterization of generated constructs

Immediately after cell seeding or following 2 weeks culture, chondrocyte-scaffold constructs were fixed in 4% formalin, embedded in paraffin, cross-sectioned and stained with Safranin-O for sulfated glycosaminoglycans (GAG). BMSC-scaffold constructs were formalin fixed after explantation following 8 weeks in ID mice, embedded in paraffin, cross-sectioned and stained with hematoxylin-eosin.

3. Results and Discussion

3.1 Development and characterization of the lower (bony) and intermediate (tidemark) layers

The selected procedure, differently from processes previously reported, implies the dispersion of collagen into the acid solution and the addition drop-wise of this mixture into the basic dispersion

so that to maintain basic condition (pH>8) for almost all the process. Under these conditions, the fibril formation takes place before the precipitation of calcium phosphate, which is crucial since the collagen fibrils are supposed to act as templates for the mineralization. Upon decrease of pH lower than ~8, amorphous HA forms onto the fibrils before their assembling into fibers. Approaching neutral pH two processes enter in competition, involving the same binding chemical groups on the surface of the fibers: the organization of collagen fibers into a three-dimensional network and the proceeding HA crystallization [13,14,19,20] .

The final porosity of the spongy mineralized composites was directly dependent on the freezing temperature, heating ramp and the content of water into the starting gel. When the freezing temperature was settled at -25°C, with a heating ramp set at 1°C/min the large pores appeared anisotropic, with the largest dimension in the range 250-450 μm (Fig. 1). Lowering of the freezing temperature up to -40°C induced a decrease of the pore diameters and an eccessive pore anisotropy [13]. By knitting the collagen/HA gel we assured the formation of macropores up to 400μm [21]. Among the several methods used to define the micro-macro porosity and the interconnectivity of the mineralized composites, XRay μCT was also employed with a local resolution of 10 μm, revealing a total porosity around 80%, a surface-to-volume ratio of 0.116 and a pore wall thickness of about 15 -20 μm.

Results of the ICP analysis of the HA/Coll composites are reported in Table 1: the different values of the Ca/P ratio of HA and Mg doped HA, nucleated on Collagen, are in the range of low crystallinity HA (~ 1.45-1.60): in fact the presence of HPO_4^{2-} in low crystallinity apatites contributes to lower the ratio. In the case of composites Mg-HA/Coll 70/30 wt%, the amount of Mg substituting Ca is exactly as expected, i.e. about 50% of the starting nominal concentration of Mg [22, 23]. On the contrary, when the inorganic/organic ratio is lowered at 40/60 HA/Coll the amount of Mg substituting Ca into HA structure decreased. The XRD analysis of HA/Coll composite displayed a pattern typical of very low crystallinity HA; the estimated crystallite size along **c** axis was around 12-15 nm. The nucleation occurred according to the process typical of natural bone, where the nano-size dimension of crystallites is responsible of the large broadening of reflections in the pattern. Such nanocrystals were growing inside collagen fibers with their **c** axes preferentially oriented parallel to the direction of orientation of the fibers [14, 24, 25]. In the case of the composite containing Mg-HA, the XRD pattern (Fig. 2) had a profile typical of amorphous phase. In the case of composites with lower inorganic/organic phase ratio (40/60) it was systematically observed that the diffraction peaks (see Fig. 2b) began to be resolved: actually in the composite with lower HA/Coll ratio, the amount of magnesium entered into the HA lattice was lower and thus the crystallinity of HA phase increased [22]. A possible explanation could be linked to the higher

affinity of Ca^{2+}, with respect to Mg^{2+}, to link COO^- groups of collagen, therefore when the HA/Col ratio is ≤ 40/60 most of the mineral phase grows in tight contact with collagen fibers and Ca^{2+} ion (instead of Mg^{2+}) preferentially binds carboxylic groups present at the surface of collagen fiber, therefore maintaining its place within the HA lattice. Differently behaves the HA phase not directly contacting the organic fibers, where the competition between magnesium and calcium is mainly controlled by the nucleation and subsequent crystallization kinetics. The complete absence of any undesirable crystalline secondary phase in all the preparations, even after a thermal treatment up to 800°C, is a further important information that can be drawn out by XRD analysis.

The mineral phase was evaluated from a typical set of HREM images (Fig. 3). The HA crystals nucleated on the organic fiber exhibited a rod like structure (Fig. 3a). When Mg^{2+} substituted Ca^{2+}, the nuclei of mineral phase had a globular shape and smaller dimensions (Fig. 3b). The inset of Fig. 3b displays at higher magnification the Mg-HA nucleus on collagen fiber. The analysis of the high resolution images and its Fourier Transform (FT) (inset c in Fig. 3b) revealed that this shape is accompanied by a lack of order and the particles appear completely amorphous, as indicated by the intense diffuse ring and by the complete lack of spots in the FT of the image. It must be stressed that the degree of disorder observed for this sample does not correspond to a short range order (as the case of low crystalline inorganic HA) but to a "true amorphous" structure [25]. These data indicate that, despite comparable synthesis conditions were used, the structural features of the mineral phase in the composite are completely different from that nucleated in the absence of an organic template [26], moreover, during mineralization, a structural control was accomplished through the preferential nucleation of a specific crystal face/axis, by molecular recognition, at the surface of the organic template. Since Mg has different polarity, structure and stereochemistry (as compared to Ca) the activation energy controlling the nucleation rate changes and this reflects in a modification of site-specificity, mineral structure and crystallographic alignment [19, 27]. Another clear evidence of the chemical interaction between HA and collagen fibers comes from the study of the FTIR spectra (Fig. 4a), in which a shift from 1340 to 1337 cm^{-1} of the band corresponding to the stretching of $–COO^-$ group of collagen, was observed. The band at 870 cm^{-1} was stronger for HA/Coll composites, indicating that the nucleation of HA into collagen implies carbonation of the inorganic phase. Moreover the carbonation can be assigned only to the B position as confirmed by the absence of the band at 880 cm^{-1} and by EDS analysis (after collagen elimination by enzymatic digestion), which revealed that the increase of the C content (in the CO_3^{2-} groups) corresponds to a decrease in P concentration. Similarly, Mg-HA nucleated on collagen results spontaneously carbonated and therefore the actual theoretical formula of the mineral phase becomes:

$$[(Ca, Mg)_{10-x/2}(PO_4)_{6-x}(CO_3)_x(OH)_2].$$

Thus, like in the natural mineralization process, it was possible to recognize also a chemical control mechanism which occurred during the nucleation and crystals growth and was mainly achieved by the regulation of ion movement and the kinetic competition between the fibrils assembling and HA nucleus formation [19]. In Fig. 4b a comparison between HA/Coll and Mg-HA/Coll is reported: normally, the low site symmetry of the PO_4^{3-} tetrahedron of crystalline HA splits the ν_4 PO_4^{3-} contour into three components which fall near 630, 600, and 550 cm^{-1}. It is possible to observe that the triplet tends to merge in two and one broad band in HA/Coll composite and Mg-HA/Coll composite respectively. In addition, the broad band centered between 550 and 560 cm^{-1}, assigned to acid phosphate (HPO_4^{2-}) in the mineral lattice, was much more intense in Mg doped HA nucleated on Collagen. These peculiarities of MgHA/Coll can be similarly observed in the FTIR spectrum of young bone; while they tend to disappear in mature bone and in highly crystalline synthetic apatite [28-30]. Correlation was noted between the fractional intensity of ~1050 cm^{-1} band related to PO_4^{3-} group and the crystal size of the apatite: a reduction of the apatitic crystal size induced an increase of the percentage area of this component [31, 32]. All these features indicate that the mineral phase containing Mg ions and nucleated on the natural template (collagen) is non-stoichiometric and remarkably amorphous resembling very well the features of newly deposited bone mineral.

Flexural strength (σ) was determined on the HA/Coll 70/30 wt% dry composites revealing a pseudo-plastic behavior. Due to technological obstacles some samples turned out extremely non-homogeneous and this is reflected in very different behavior under loading. The flexural strength decreased from about 20 to 5 MPa as the specimen porosity increased from about 45 to 63 vol% (Table 2). From the regression curve of the strength and porosity data, the equation:

$$y = 330.5\ e^{-6.8481x}$$

was derived and σ value at zero porosity was also calculated (= 330 MPa), that can be considered an approximation of the strength of the material at full density). Elastic modulus (Young's modulus - E) determined on the mineralized layer well reproduced the value found for trabecular bone at correspondent values of porosity (Table 2).

3.2 Development and characterization of the upper cartilagineous layer

The pure collagenic portion (mimicking cartilage) was added with hyaluronic acid to create bridges between the collagen fibers and, through the introduction of this saccharidic structure rich in polar hydrogen atoms, to modify the hydrophilicity of the system. In Fig. 5 the ESEM image shows the details of the hyaluronic acid bridges. The porosity of the cartilagineous layer is visible in the inset of Fig. 5 and was evaluated by image analysis: the pores result more isotropic if compared with the mineralized composite and the average pore diameter was in the range of 100-150 μm. Solid state

NMR analysis was performed on the collagenic (cartilaginous) layer with and without hyaluronic acid to confirm its presence (Fig. 6), while detailed quantitative analysis are in progress.

BDDGE (1,4-butanediol diglycidyl ether) was added to the three different layers as cross linking agent to stabilize collagen and retard its degradation kinetic. However the effect of the cross-linking agent on the material morphology is more evident on collagen when the mineral phase is absent. A comparison between the morphology of the freeze dried collagen and freeze dried collagen + BDDGE is shown is Fig. 7, highlighting the different morphology induced by BDDGE and the higher number of links between the collagen bundles in the cross-linked sample. Enzymatic tests carried out on the different layers using Collagenase revealed that the mineral phase retards the degradation of collagen and BDDGE further stabilizes the HA/Coll composite: HA/Coll 70/30 wt% degraded completely in 38hrs, while HA/Coll 70/30 wt% + BDDGE in 78hrs. On the other hand, Collagen/Hyaluronic Acid degraded in 3.5hrs while Collagen/Hyaluronic Acid + BDDGE in 7hrs. A more detailed description of tests and the nature of link formed between collagen and BDDGE in function of pH will be discussed in a following paper.

3.3 Development and test of the three-layered scaffold

The rationale to fabricate a three-layered scaffold instead of a bi-layered one is based on the consideration that gradual changes in the mechanical features of the layers, due to different stiffnesses of the differently mineralized fibers, could reduce the mismatch of properties at the interface and increase the composite stability. Fig. 8 displays the ESEM image of the graded composite: it is possible to distinguish a disordered lower layer that corresponds to the mineralized one, a second layer, with lower mineralization extent, which corresponds to the tidemark and a third layer in which the propagation of a planar ice front [33] during a freeze-dry cycle, causes the formation of a columnar-like structure converging towards the external surface where it forms horizontal flat ribbons, resembling the morphology of the *lamina splendens*. In the lower layer, the higher density and scarce flexibility of the mineralized fibers hamper the formation of a directionally ordered structure during freeze-drying. Pulling tests on dry and wet samples were manually performed and the detaching interfaces evaluated: in a statistically significant number of tests the separation occurred in a random position (not at the layers interface), proving that the knitting procedure assures a good adhesion between the mineralized layers and the cartilagineous one.

Chondrocytes statically loaded in the composite scaffolds remained mostly confined within the seeded layer and their distribution within the layer was rather non-uniform (Fig. 9 a, b). Cells appeared more sparse and at lower density in the subchondral bone than in the cartilaginous layer.

After 2 weeks in *chondrogenic medium*, cells in the cartilaginous layer displayed a chondrocytic morphology and generated a cartilaginous tissue positively stained for Safranin O (Fig. 9c), while cells in the subchondral bone layer remained fibroblastic and did not accumulate histologically detectable amounts of glycosaminoglycans (Fig. 9d). The scaffold regions initially void of cells, especially those in the central core, remained essentially acellular (data not shown). After 8 weeks in ID mice, BMSC loaded in the composite scaffold generated a nicely structured bone tissue confined in the bone layer and a loose connective tissue in the cartilagineous layer (Fig. 10).

The obtained results demonstrate that the cartilaginous layer of the composite scaffold is permissive to human articular chondrocyte differentiation and cartilaginous matrix deposition, whereas only a fibrous tissue could develop in the subchondral bone layer. Conversely, bone tissue formation was supported within the subchondral layer of the composite, but not in the cartilaginous region. Further studies are required to establish whether the differential tissue formation is due to the initially different density of seeded cells, to the different architecture of the layers (e.g., pore size) or to effectively biomimetic cues in their composition (e.g., hydroxyapatite, hyaluronic acid component). The role of 3-layered composites, as compared to 2-layered structures, will also have to be addressed in orthotopic animal models.

4. Conclusions

HA/Coll bio-hybrid composites were prepared through a biologically inspired mineralization process. The presence of magnesium, doping hydroxyapatite nucleating on collagen (Mg-HA/Coll), induces in the composite those physico-chemical, structural and morphological features typical of newly formed natural bone. Actually, during the artificial mineralization process, intrinsic control mechanisms such as regulation of chemistry, morphology and spatial distribution of the mineral phase occur, similarly to what happens in natural biomineralization process. Compositionally and morphologically graded scaffolds, made with the bio-hybrid composites, displayed the ability to support selective cell differentiation towards the osteogenic and chondrogenic lineages. Further studies are ongoing to test whether the biomimetic properties of the graded scaffold can induce orderly repair of osteochondral defects in a large size animal model.

References

1. Buckwalter JA, Woo SL, Goldberg VM, Hadley EC, Booth F, Oegema TR et al. Soft-tissue aging and musculoskeletal function. J Bone Joint Surg 1993;75:1533-1548.

2. Hutmacher DW. Scaffolds in tissue engineering bone and cartilage. Biomaterials 2000;21:2529-2543.

3. Hutmacher DW, Zein I, Teoh SH, Ng KW, Schantz JT, Leahy JC. Design and fabrication of a 3D scaffold for tissue engineering bone. In: Agrawal CM, Parr JE, Lin ST, editors. Synthetic bioabsorbable polymers for implants, STP 1396. American Society for Testing and Materials. West Conshohocken: PA, 2000. p.152-167.

4. Martin I, Obradovic B, Treppo S, Grodzinsky AJ, Langer R, Freed LE et al. Modulation of the mechanical properties of tissue-engineered cartilage. Biorheology 2000;37:141-147.

5. Martin I, Miot S, Barbero A, Jakob M, Wendt D. Osteochondral tissue engineering. J Biomech 2007;40(4):750-765.

6. Newman AP. Articular cartilage repair. Am J Sports Med 1998;26:309-324.

7. Bernhardt A, Lode A, Boxberger S, Pompe W, Gelinsky M. Mineralised collagen-an artificial, extracellular bone matrix-improves osteogenic differentiation of bone marrow stromal cells. J Mater Sci: Mater Med. 2007; DOI 10.1007/s10856-006-0059-0.

8. Domaschke H, Gelinsky M, Burmeister B, Fleig R, Hanke T, Reinstorf A, et al. In vitro ossification and remodeling of mineralized collagen I scaffolds. Tissue Eng 2006;12(4): 949-958.

9. Gelinsky M, Eckert M, Despang F. Biphasic, but monolithic scaffolds for the therapy of osteochondral defects. Int J Mater Res 2007;8:749-755.

10. Yokoyama A, Gelinsky M, Kawasaki T, Kohgo T, Konig U, Pompe W et al. Biomimetic porous scaffolds with high elasticity made from mineralized collagen-an animal study. J Biomed Mater Res 2005;75B:464–472.

11. Sherwood JK, Susan LR, Palazzolo R, Brown SC, Monkhouse DC, Coates M et al. A three-dimensional osteochondral composite scaffold for articular cartilage repair. Biomaterials 2002; 23: 4739–4751.

12. Scheck RM, Taboas JM, Segvich SJ, Hollister SJ, Krebsbach PH. Engineered osteochondral grafts using biphasic composite solid free-form fabricated scaffolds. Tissue Eng 2004; 10:1376-1385.

13. Gelinsky M, Welzel PB, Simon P, Bernhardt A, Konig U. Porous three-dimensional scaffolds made of mineralized collagen: preparation and properties of a biomimetic nanocomposite material for tissue engineering of bone. Chem Eng J 2007; DOI:10.1016/j.cej.2007.09.029.

14. Tampieri A, Celotti G, Landi E, Sandri M, Roveri N, Falini G. Biologically inspired synthesis of bone like composite: self assembled collagen fibers/hydroxyapatite nanocrystals. J Biomed Mater Res. 2003;67A:618-625.

15. Serre CM, Papillard M, Chavassieux P, Voegel JC, Boivin G. Ifluence of magnesium substitution on a collagen-apatite biomaterial on the production of a calcifying matrix by human osteoblasts. J Biomed Mater Res 1998; 42: 626-633.

16. Liu C, Xia Z. Design and development of three-dimensional scaffolds for tissue engineering. Pharm Eng 2007;85:1051-1064.

17. Barbero A, Grogan S, Schäfer D, Heberer M, Mainil-Varlet P, Martin I. Age related changes in human articular chondrocyte yield, proliferation and post-expansion chondrogenic capacity. Osteoarthritis and Cartilage 2004;12:476-484.

18. Mastrogiacomo M, Scaglione S, Martinetti R, Dolcini L, Beltrame F, Cancedda R, et al. Role of scaffold internal structure on in vivo bone formation in macroporous calcium phosphate bioceramics. Biomaterials 2006;27:3230-3237.

19. Mann S. Biomineralization. Principles and Concepts in Bioinorganic Materials Chemistry. Oxford University Press: CH 3-6, 2001. p 24-124

20. Bradt JH, Mertig M, Teresiak A, Pompe W. Biomimetic mineralization of collagen by combined fibril assembly and calcium phosphate formation. Chem Mater 1999;11:2694-2701.

21. Patent WO/1995/025482. Three-dimensional bioremodelable collagen fabrics.

22. Landi E, Tampieri A, Mattioli-Belmonte M, Celotti G, Sandri M, Gigante A et al. Biomimetic Mg- and Mg, CO_3- substituted hydroxyapatites: synthesis, characterization and in vitro behaviour. J Eur Ceram Soc 2006;26:2593-2601.

23. Tampieri A, Celotti G, Landi E, Sandri M. Magnesium doped hydroxyapatite, synthesis and characterization. Key Eng Mater 2004;264–268:2051–2054.

24. Roveri N, Falini G, Sidoti MC, Tampieri A, Landi E, Sandri M et al. Biologically inspired growth of hydroxyapatite nanocrystals inside self-assembled collagen fibers. Mat Sci Eng 2003;C23:441-446.

25. Bertinetti L, Tampieri A, Landi E, Sandri M, Martra G, Coluccia S. Biomaterials at nanoscale: morphology and surface structure of nanosized hydroxyapatite. Nanoparticles, Nanostructures and Nanocomposites, EcerS 2004 Topical Meeting, Saint Petersburg 5-7 July 2004

26. Celotti G, Tampieri A, Sprio S, Landi E, Bertinetti L, Martra G et al. Crystallinity in apatites: how can a truly disordered fraction be distinguished from nanosize crystalline domains? J Mater Sci: Mater Med 2006;17:1079–1087

27. Bertinetti L, Tampieri A, Landi E, Martra G, Coluccia S. Punctual investigation of surface sites of HA and magnesium-HA. J Eur Ceram Soc 2006; 26: 987-991.

28. Rey C, Shimizu M, Collins B, Glimcher MJ. Resolution-enhanced Fourier transform infrared spectroscopy study of the environment of phosphate ions in the early deposits of a solid phase of calcium-phosphate in bone and enamel, and their evolution with age. I: Investigations in the ν_4 PO_4 domain. Calcif Tissue Int 1990;46:384-394.

29. Fowler BO, Moreno EC, Brown WE. Infra-red spectra of hydroxyapatite, octacalcium phosphate and pyrolysed octacalcium phosphate. Arch Oral Biol 1966;11:477-492.

30. Miller LM, Vairavamurthy V, Chance MR, Mendelsohn R, Paschalis EP, Betts F et al. In situ analysis of mineral content and crystallinity in bone using infrared micro-spectroscopy of the ν_4 PO_4^{-3} vibration. Biochim Biophys Acta 2001;1527:11-19.

31. Paschalis EP, DiCarlo E, Betts F, Sherman P, Mendelsohn R, Boskey AL. FTIR microspectroscopic analysis of human osteonal bone. Calcif Tissue Int 1996;59:480-487.

32. Pleshko N, Boskey A, Mendelsohn R. Novel infrared spectroscopic method for the determination of crystallinity of hydroxyapatite minerals. Biophys J 1991;60:786-793.

33. Schoof H, Apel J, Heschel I, Rau G. Control of pore structure and size in freeze-dried collagen sponges. J Biomed Mater Res 2001;58B:352–357.

Captions

Figure captions

Figure 1: SEM image of the mineralized bony layer made of 70/30 wt% HA/Coll

Figure 2: X ray diffractogram of MgHA/Coll (70/30)wt (a), MgHA/Coll (40/60)wt (b)

Figure 3: Set of HREM images: TEM micrography of freeze milling HA/Coll (70/30)wt composite (a) and TEM micrography of freeze milling MgHA/Col (70/30)wt composite (b). Insert (c): high resolution HREM images and Fourier Transform.

Figure 4 : FTIR analyses of apatite/Collagen composites containing different mineral phases (HA, MgHA) compared with crystalline HA (a) and detail of PO_4 peak area comparison (b).

Figure 5: ESEM micrography of the morphology of the cartilaginous layer made of collagen containing Hyaluronic acid

Figure 6: Solid State NMR analysis : freeze dried collagen (a) and freeze dried collagen with Hyaluronic Acid added (b).

Figure 7: ESEM micrography of freeze-dried natural collagen (a) and BDDGE cross-linked collagen (b).

Figure 8 ESEM micrography of osteochondral scaffold morphology: three different layers are distinguishable due to the different content of mineral phase, that increases moving from the upper (cartilagineous: collagenic only) to the intermediate (tide-mark: HA/Coll 40/60wt composite), to the lower layer (bone layer: HA/Coll 70/30wt composite). The inset shows the detail of the morphology of cartilaginous (upper) layer: a columnar-like structure converges towards the external surface where it forms horizontal flat ribbons, resembling the morphology of the *lamina splendens*.

Figure 9 Representative safranin O-stained cross-sections of constructs after seeding (a,b), or following two weeks of culture in chondrogenic medium (c,d) of scaffolds seeded from the cartilaginous layer (a,c) or from the subchondral bone layer (b,d). Scale bar = 100 μm (or 50 μm for the inset in c)

Figure 10: Histological characterization of BMSC generated constructs. The histological analysis of BMSC loaded constructs retrieved after 8 weeks of in vivo implantation in ID mice revealed a nicely formed bone tissue limited to the construct bone layer (upper part of the panel) and a loose connective tissue in the construct cartilagineous layer (lower part of the panel). The dotted line underlines the transition between bone and cartilage layers of the construct. Staining Hematoxylin-Eosin.

Figure

Click here to download high resolution image

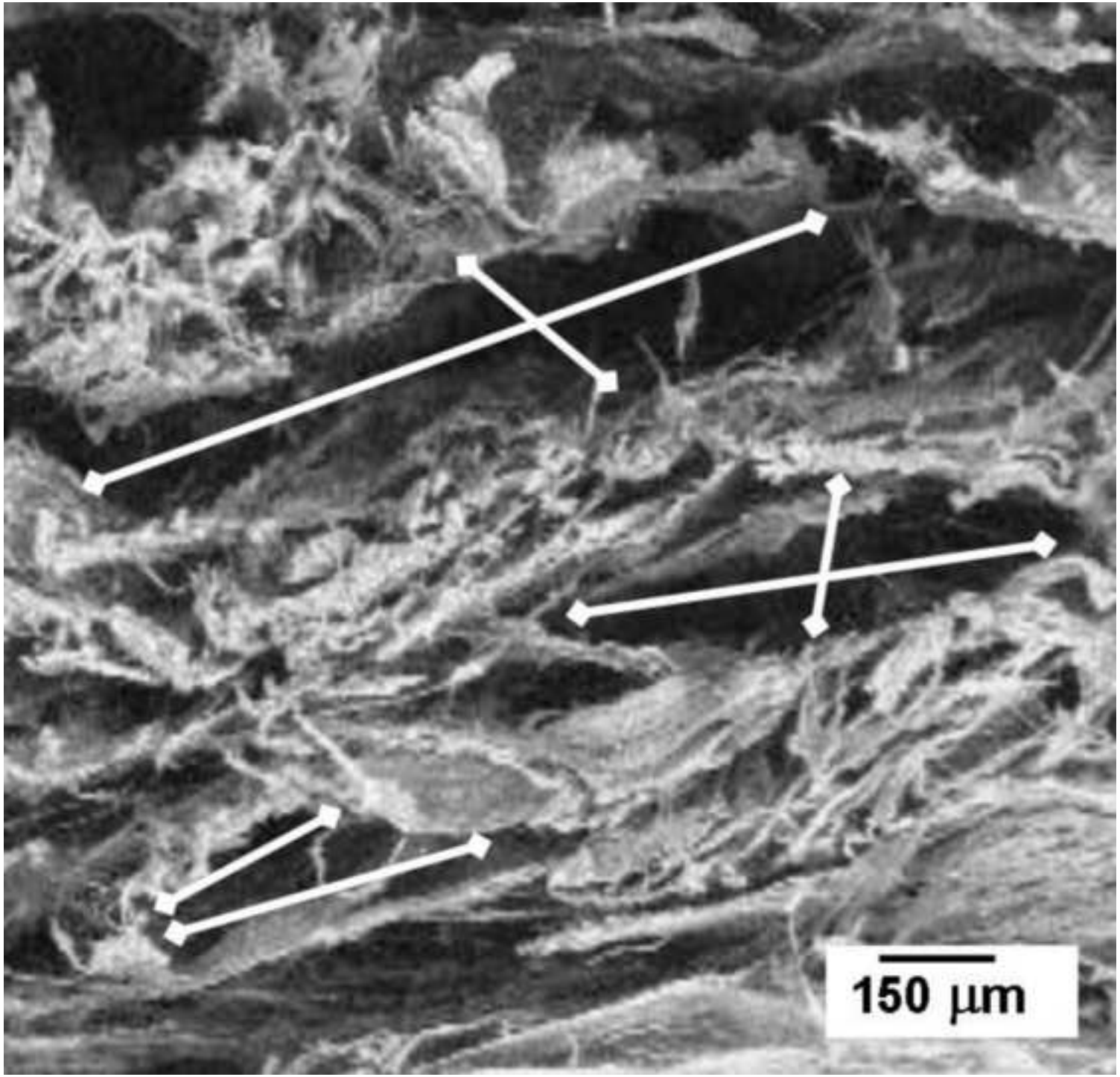

Figure

Click here to download high resolution image

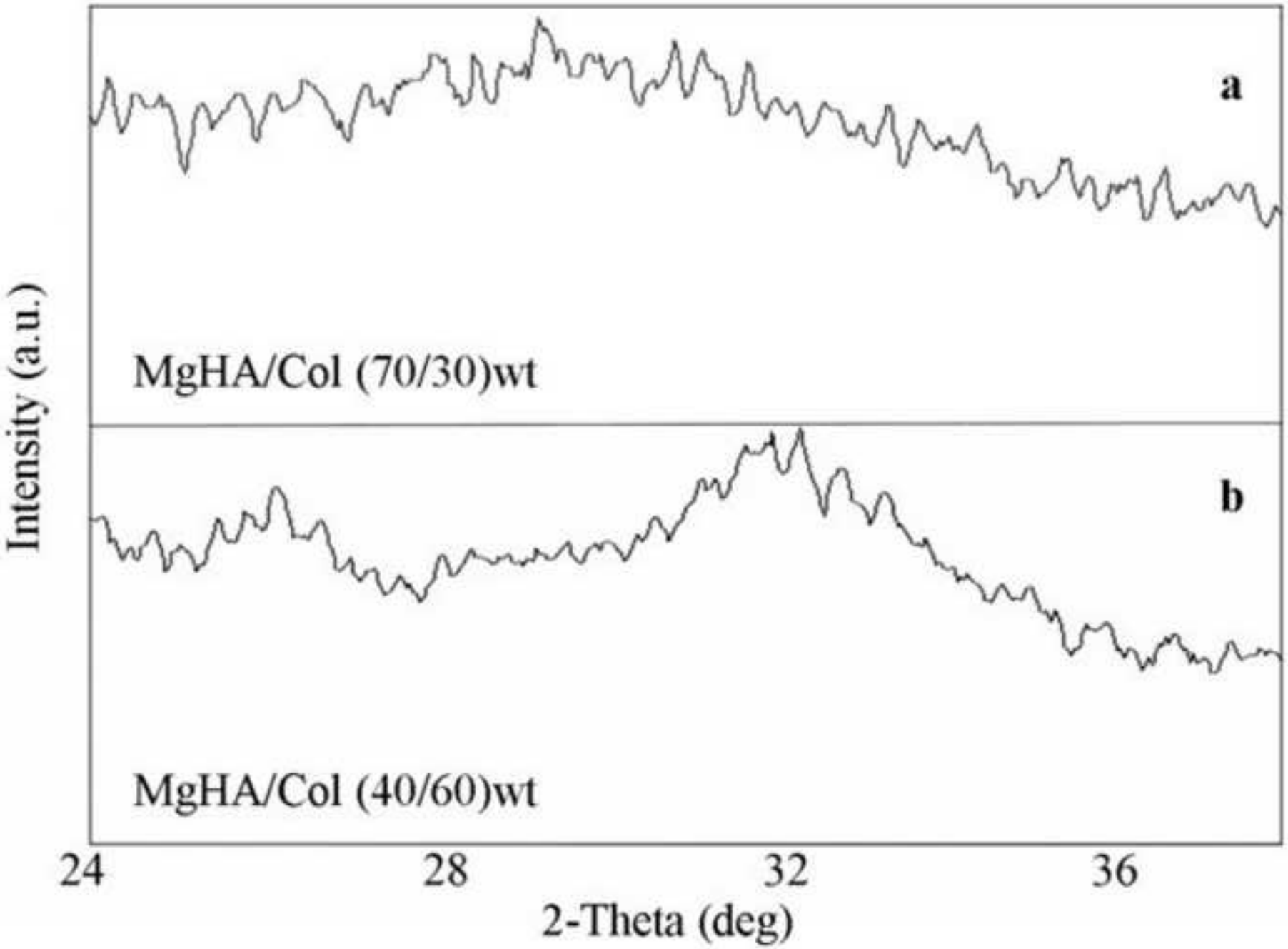

Figure

Click here to download high resolution image

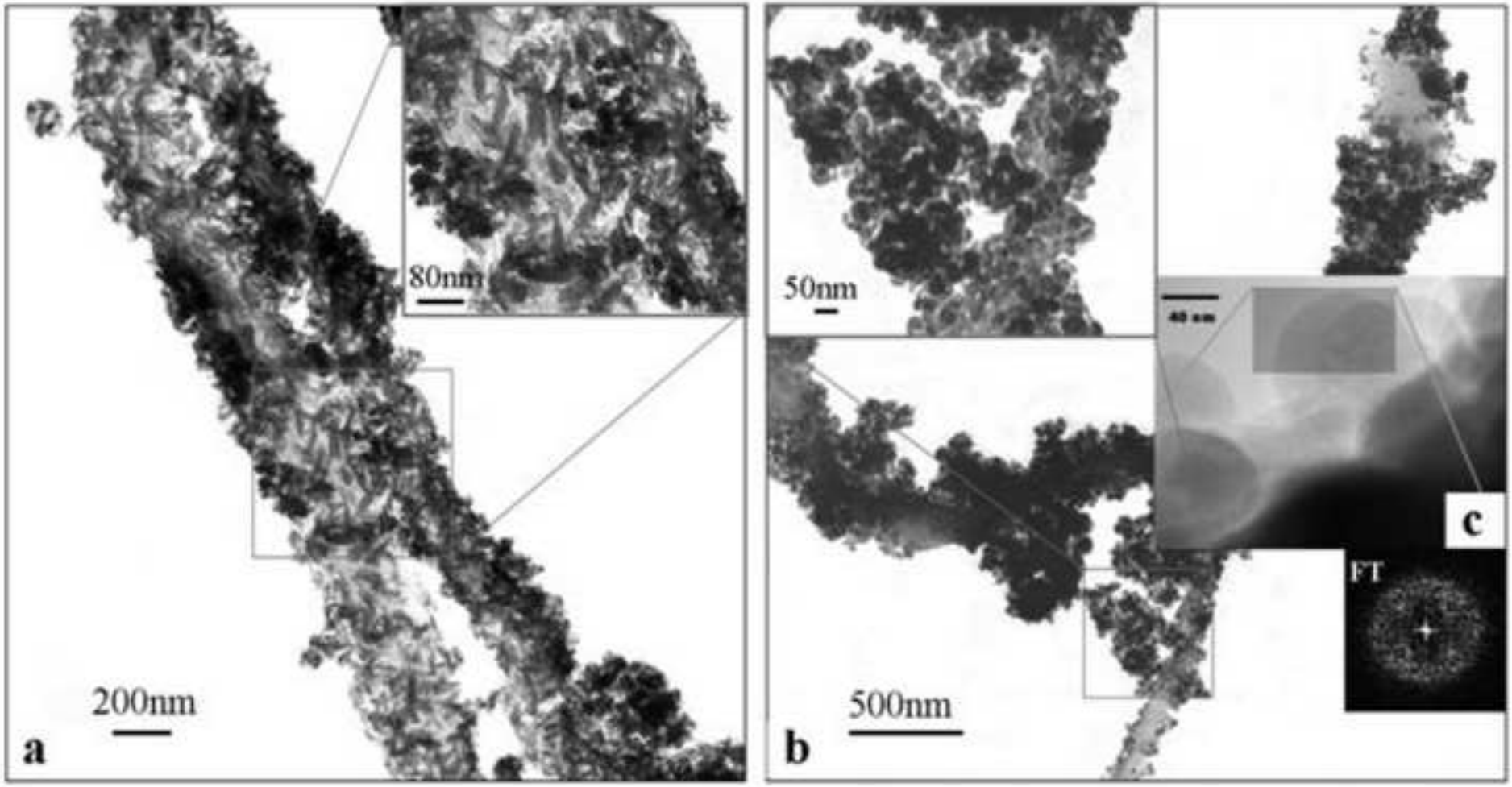

Figure

Click here to download high resolution image

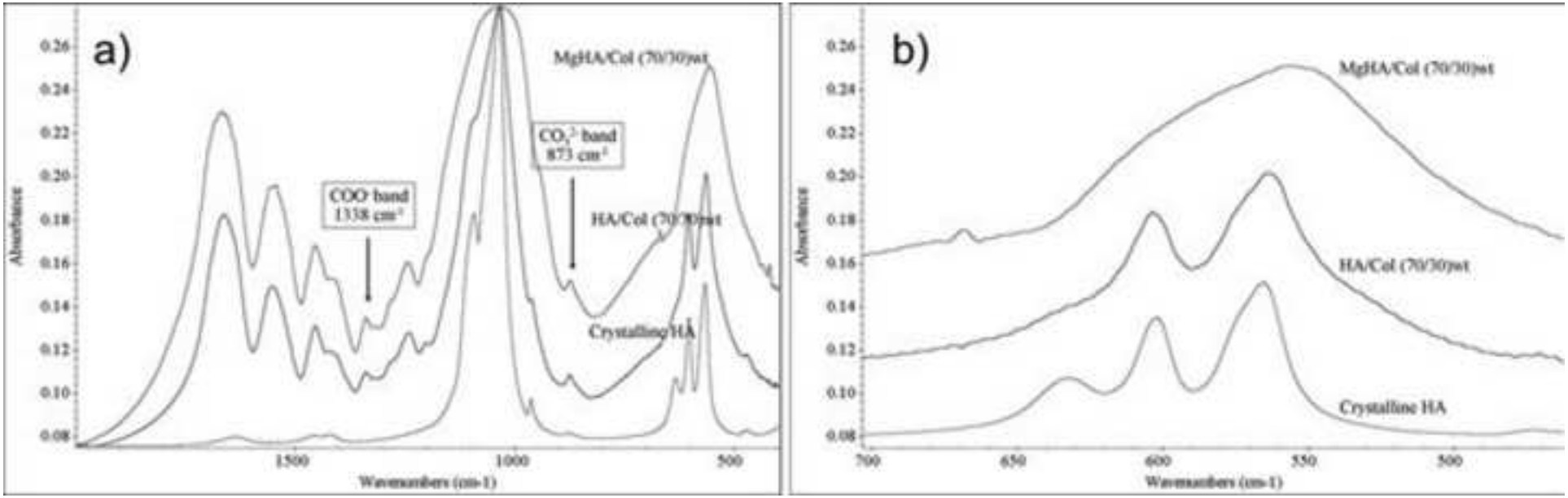

Figure

Click here to download high resolution image

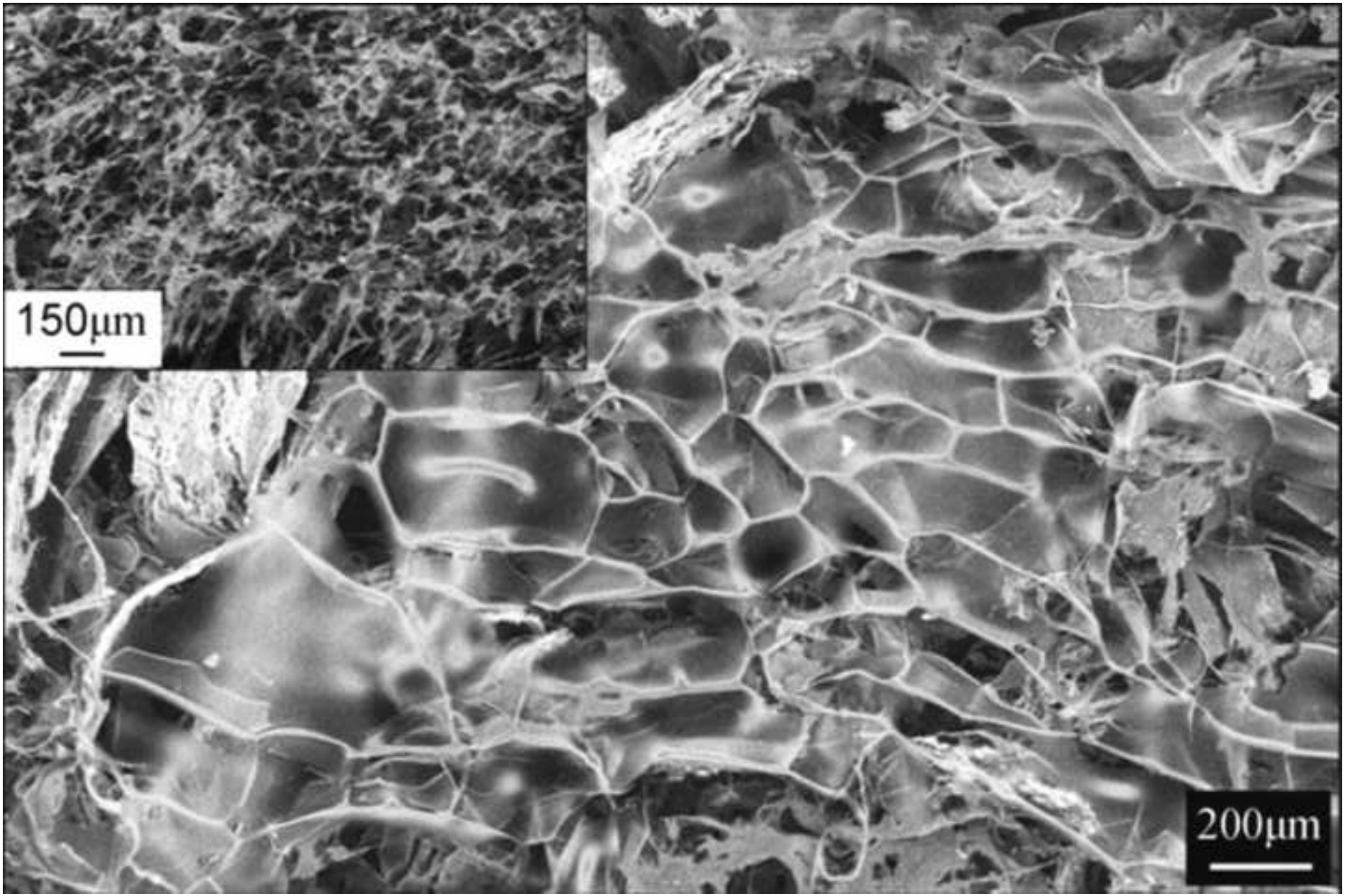

Figure

Click here to download high resolution image

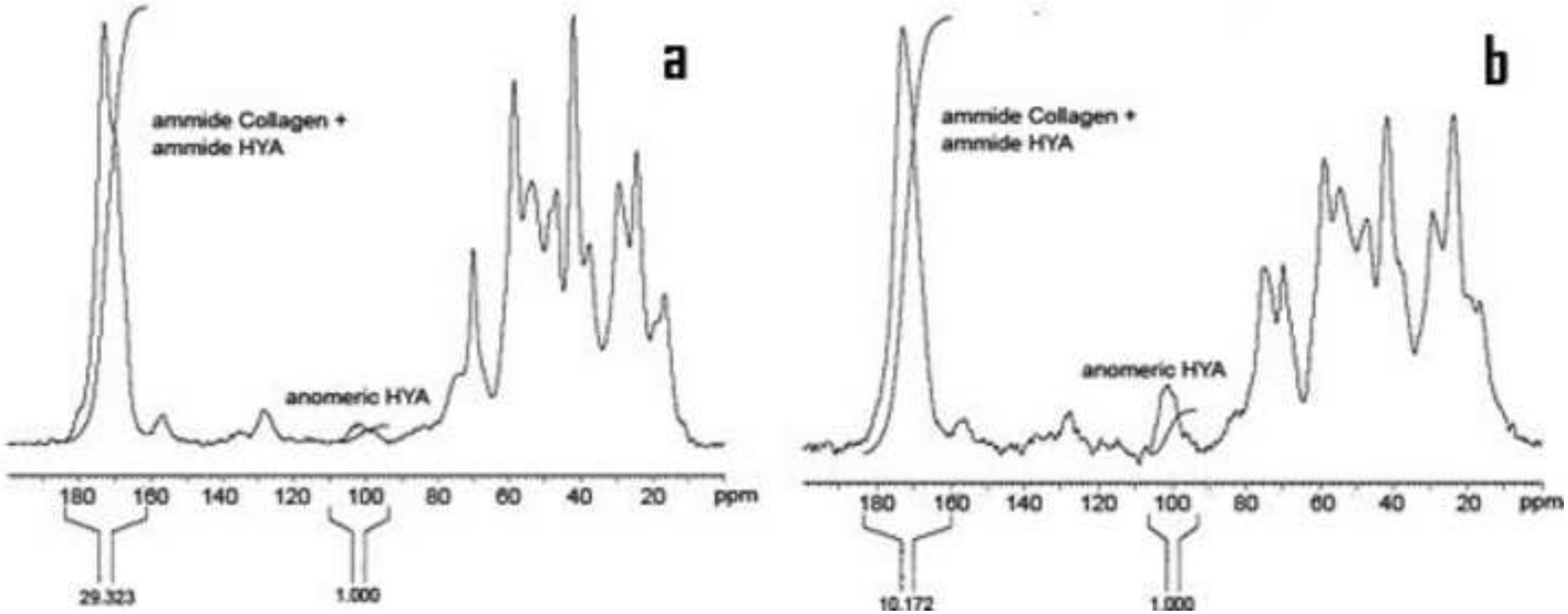

Figure

Click here to download high resolution image

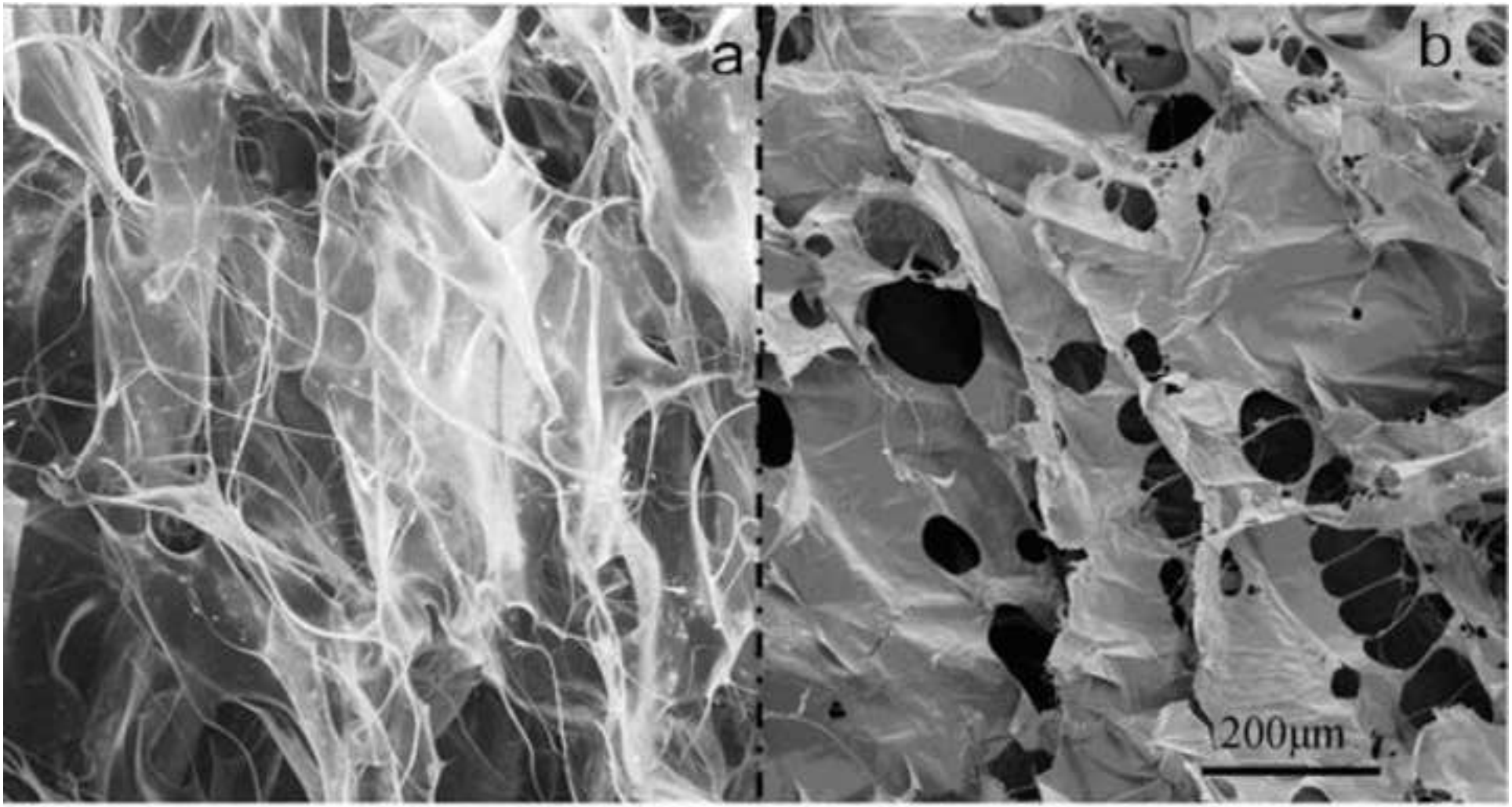

Figure

Click here to download high resolution image

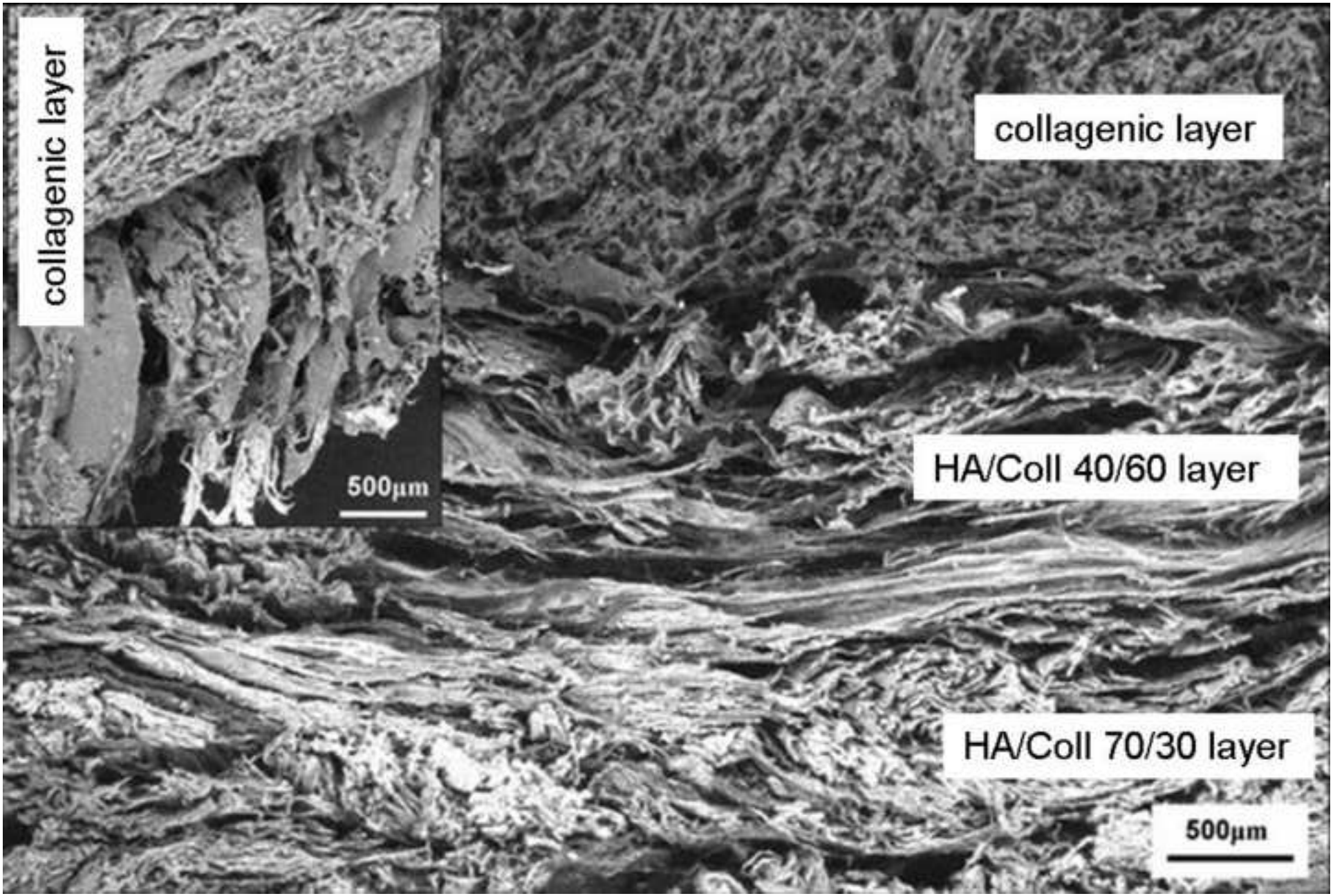

Figure

Click here to download high resolution image

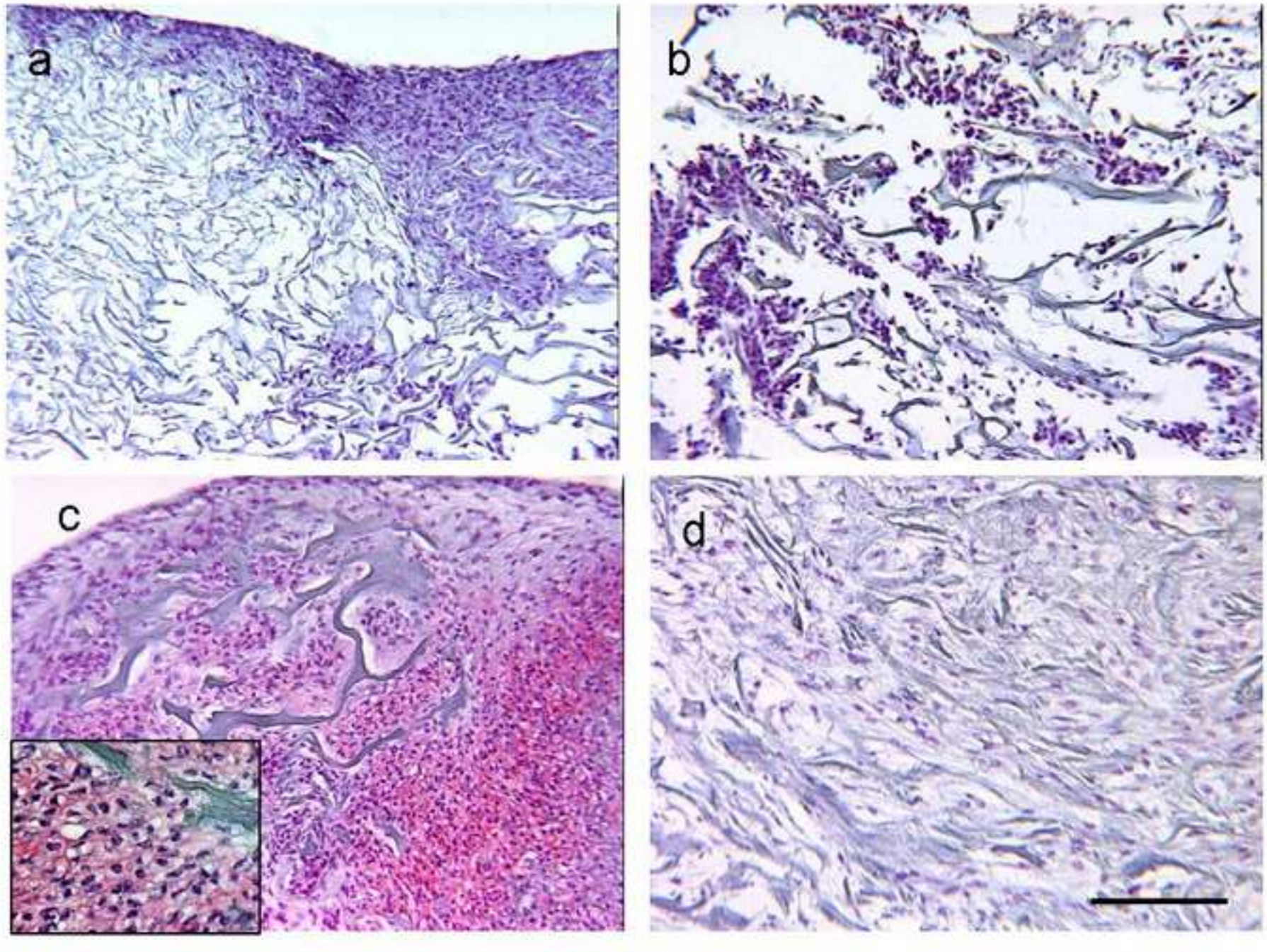

Figure

Click here to download high resolution image

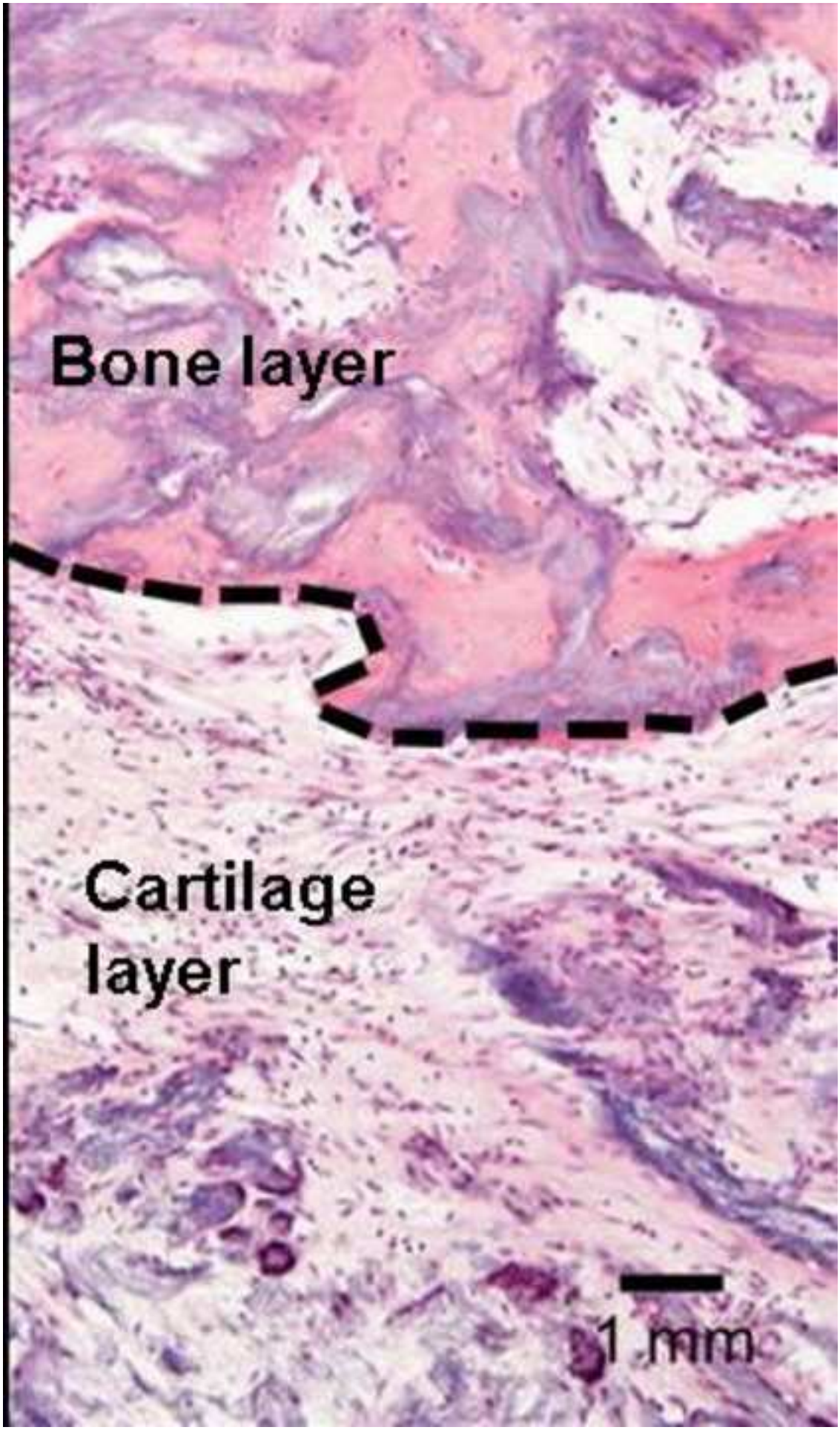

Table

Table 1: ICP-OES quantitative analyses of apatite/collagen composites.

	Ca^{2+} (mol)	Mg^{2+} (mol)	PO_4^{3-} (mol)	Molar Ca/P	Molar (Ca+Mg)/P	Molar Mg/Ca (%)
HA / Coll (70/30)wt	1.870	---	1.144	1.635	---	---
MgHA / Coll (70/30)wt	1.315	0.035	0.857	1.534	1.575	2.662
MgHA / Coll (40/60) wt	1.419	0.027	0.983	1.444	1.471	1.903

Table

Table 2: Flexural strength (σ) values (three point bending method for flexural strength evaluation) and Young's modulus (E) values obtained for HA/Coll 70/30 bars having different porosity value (in the range 45-65 %).

Specimen porosity (%)	Flexural strength σ (MPa)	Young's modulus E (GPa)
45.3	17.56	6.85
45.9	23.23	4.51
46.7	7.46	6.29
51.5	7.86	3.44
52.4	8.77	2.00
54.1	9.05	3.91
62.0	4.68	1.81
62.6	4.92	1.65
63.3	6.11	1.50